Utilization of Waste CO_2 Generated Vaterite in Blended Cements

Ying Wang [1], Jesus Gonzalez [1], Craig W. Hargis [1,*]

[1] Fortera Corporation, 100 Great Oaks Blvd suite 120, San Jose, CA 95119

* Correspondence: chargis@forterausa.com

Dr. **Ying Wang** is a Scientist at Fortera in San Jose, CA. She is a member of ACI Committees 232-00 (Fly Ash and Bottom Ash in Concrete) and 88-S806 (Young Member Activities). She obtained her Ph.D. degree in Civil Engineering in 2022. Her research interests encompass sustainable cement development, supplementary cementitious materials reactivity evaluation and utilization, and blended cements performance design.

ACI member **Jesus Gonzalez** is an Engineer at Fortera in San Jose, CA. He graduated from Universidad Autonoma de Nuevo Leon with a master's degree in Traffic and Road Engineering in 2019. He specializes in ready-mix concrete production and utilization.

Dr. **Craig W. Hargis** is a materials scientist with extensive experience in construction materials, reduced carbon intensity cements, composites, novel inorganic binders, and durability. Craig is the vice president of products at Fortera, which he joined in 2020. He was previously an Assistant Professor at the University of North Florida in the Construction Management Department. Prior to that he was a researcher at EMPA, Calera, the University of California at Berkeley, and the University of Texas at Austin.

Synopsis: This paper discusses the results of a 5-10% vaterite replacement of SCMs in certain blended cements. In a cement-fly ash blended cement, a 10% vaterite replacement of fly ash achieved a 40% higher strength at 1 day and maintained a consistently higher strength than the cement-fly ash blended cement control through 56 days. A 10% vaterite replacement of slag in a cement-slag blended cement achieved approximately 20% higher strength at 3 days. For a cement-slag-fly ash blended cement, a 10% replacement of fly ash with vaterite achieved a 30% to 50% strength increase through 7 days, and a 50 to 110-minute reduction in initial setting. The bulk resistivity of all the blended cements were increased after including vaterite, indicating the potential for better durability. The alkali silica reaction test resulted in low amounts of expansion confirming the vaterite blended cements' durability. Hydration analysis using isothermal calorimetry and thermogravimetry also showed extra early-age hydration reactions due to vaterite inclusion. Using vaterite in blended cements can help reduce the embodied carbon and enhance many of the engineering properties, such as setting time, early-age strength, and durability.

Keywords: cement, early age strength, setting time, sustainability, vaterite

INTRODUCTION

Cement production is responsible for 7-8% of all anthropogenic CO_2 emissions, over 3% of global energy demand, and over 5% of global anthropogenic PM_{10} emissions [1]. With the megatrends of increasing global population and urbanization, these environmental impacts will not decrease if mitigation applications are not adopted. In recent years, various technical measures were found to alleviate these impacts. For example, the CO_2 in the waste gas from the cement kiln and fossil fuels incinerator can be collected for carbonation curing, secondary chemical reactions for carbon capture, geological storage, etc. [2]. But these measures often have technical and economic challenges for application in cement plants. Another way to effectively reduce the CO_2 from the cement industry is to reduce the cement quantities required, by using supplementary cementitious materials (SCMs) or fillers in blended cement with optimized mixture proportions [2]. Blended cements such as portland-limestone cement, portland-pozzolan cement which include fly ash, natural pozzolan, or calcined clay, and ternary blended cement that may contain pozzolan, slag, or calcium carbonate have been increasingly used over the past decades [3]. The blended cements may offer extra hydration or pozzolanic reactions, and can often achieve better fresh and hardened properties among different ages [3–6]. However, the usage of SCMs in blended cement can also cause unwanted issues [7]. For instance, calcined clay typically causes a higher water demand in blended cements [7]. To enhance the workability of calcined clay blended cements, superplasticizers are often required, which may raise the cost of producing the cement or resulting concrete [8,9]. The use of fly ash in blended cements will often extend their setting times and reduce early-age strength [10]. When the cement replacement level is higher, lower-clinker factor cements often have longer set times and lower early-age strengths. Proper formulation of blended cements can address some of these issues at a low cost. The optimal use of SCMs in blended cement can potentially achieve about a 44% reduction in CO_2 emissions by the cement industry [1] and is facilitated by different standards organizations, such as ASTM or AASHTO in the United States and CEN in Europe. However, the availability of many SCMs, such as fly ash and slag, is dwindling due to the termination of coal-fired power plants and changing steel manufacturing processes around the world, necessitating the exploration of alternative materials to blend with cement [10,11].

Limestone has long been used in the cement industry, with the major $CaCO_3$ component as calcite. Portland cement often contains up to 5% calcium carbonate, and portland-limestone cement can contain up to 15-35% calcium carbonate. Adding or co-grinding calcium carbonate into cement not only offers more nucleation sites for C-S-H gel to grow on, but also contributes to the chemical and hydration reactions [3–5]. The physical nucleation effect, shearing effect [12], and improved packing offered by the calcium carbonate additions accelerate cement hydration, and the reaction between calcium carbonate and aluminates forms carboaluminates as extra hydration products, which contribute to the strength and durability of the cement [4,13]. The reaction between carbonate ions and aluminates makes fine calcium carbonate a potential material for co-substitution with aluminosilicate-based SCMs, such as fly ash, slag, and calcined clay, in blended cements [14]. Calcite is the major mineral phase of limestone, and the other two anhydrous polymorphs of calcium carbonate are aragonite and vaterite. Vaterite can be generated using CO_2 from cement kilns. It is cementitious on its own when mixed with water, and it can also be used as a supplementary material for blended cements. Vaterite is a less stable and more soluble polymorph and rarely exists in nature, whereas calcite and aragonite are the most common crystalline polymorphs. Vaterite is often used for the food industry and biomedical applications due to its higher specific surface area, higher solubility and higher dispersion compared to the other two polymorphs [15]. Several synthesis methods have been reported for vaterite production, such as CO_2 bubbling, reverse emulsion, and solution precipitation [16]. Feng et al. created vaterite by aerating a $Ca(OH)_2$ and L-Leucine mixed solution with CO_2 [17]; Mehdizadeh et al. used a two-step leaching-carbonation process to dissolve the recycled concrete fines and later carbonated the leachate to form vaterite [15]; Hargis et al. used CO_2-containing flue gas and carbide lime sludge to produce vaterite and reported the mechanical properties of the $CaCO_3$ cement made by vaterite. $CaCO_3$ cement paste can achieve 40 MPa ultimate strength after 3 days of curing at 80°C [18]. In addition to vaterite being cementitious on its own when mixed with water [18,19], it can also be used as a supplementary material for blended cements [20–22]. Zhao et al. found that cement paste with vaterite had the lowest porosity among the three polymorphs, caused by a higher solid volume formation with vaterite inclusion than calcite or aragonite [23]. Other studies used vaterite as an internal curing agent due to its porous structure and showed reduced autogenous shrinkage of mixtures with vaterite inclusion [23–25].

This paper discusses the use of vaterite in blended cements, and the results and benefits of a 5-10% vaterite replacement of SCMs in certain blended cements are presented. Characterization methods such as isothermal calorimetry (IC) and thermogravimetric analysis (TGA) were carried out to study the blended cement paste hydration, before and after the inclusion of vaterite. Fresh properties including mortar flow and setting time, and hardened properties including mortar compressive strength, bulk resistivity, and durability are reported at various ages and compared between cement blends that included 5-10% vaterite and those that did not.

MATERIAL AND METHODS

Materials

Commercial ASTM C150 Type II-V cement, low calcium fly ash, and slag and laboratory synthesized vaterite were used in this study. The vaterite synthesis process was described previously [18,26,27]. Lime (CaO) was dissolved in an aqueous solution of NH_4Cl near standard state conditions. The resulting aqueous solution containing $CaCl_2$ was contacted with CO_2 gas to produce vaterite and to regenerate the NH_4Cl. The solid was dewatered and dried to produce the final vaterite product and the solution containing NH_4Cl was recycled to the dissolution step [28]. Measured by a Bruker D8 Endeavor X-ray powder diffraction analyzer, the vaterite used in this study was 97.1% pure with a 2.9% calcite impurity. The cement had 62% C_3S, 12% C_2S, 5% C_3A and 11% C_4AF as its main mineral phases. The fly ash had a 66.3% amorphous content, with mullite and quartz being its major crystalline phases. And the slag had a 78.9% amorphous content, with alite and anhydrite being its major crystalline phases. Fig. 1 shows the morphology of the vaterite particles under SEM. Vaterite particles showed a spherical shape with a textured surface. The particles were agglomerations of many microplates and lenses showing a rosette mesostructure. The loss on ignition (LOI) of the raw materials were determined using TGA, and the median particle size (d_{50}) was measured using a Partica LA-960 laser scattering particle size distribution analyzer. The refractive index of 1.7 was used for measuring the cement PSD in isopropyl alcohol (IPA), and the refractive index of 1.58 was used for vaterite in water. The density of the raw materials was determined by a Micromeritics gas pycnometer, and the surface area of the raw materials was determined using an Anton Paar Nova 800 physisorption Analyzer. These characterization results are listed in Table 1.

Mixture proportions

Hydration analysis was carried out on paste samples using isothermal calorimetry and TGA. Hardened properties, such as compressive strength and bulk resistivity, were evaluated on mortar cubes proportioned according to ASTM C109. Durability testing for alkali silica reaction (ASR) was performed on mortar bars. For mortar bars in the ASTM C1567 accelerated mortar bar test (AMBT), the water-to-binder ratio (w/b) was fixed at 0.47, and the sand-to-binder ratio (s/b) was fixed at 1.90. Graded borosilicate glass was prepared as the reactive aggregate in line with the ASTM C1567 grading requirements. Hydration analysis was performed on cementitious pastes, using a fixed w/b of 0.6. Mortar flow was measured according to ASTM C1437. The blended cements' setting times were evaluated on normal consistency pastes according to ASTM C191. The SCMs and vaterite were used to partially replace 25–70% of the cement in the mixtures by mass. Tables 2 to 4 give the detailed mixture proportions of the tested materials, together with the mortar flow values.

Methods

Isothermal calorimetry - The heat of hydration of cementitious paste mixtures was measured using a TAM Air isothermal calorimeter. 20 g of dry powder was mixed homogeneously in a beaker with a spatula by hand for 2 min, then 12 g of deionized water was added into the powder. The wet paste was mixed using a spatula in a beaker for 2 minutes due to the small sample size. Then, approximately 10 g of the paste was transferred into a glass ampoule. After all 8 samples were loaded and sealed in the ampoules, the ampoules were lowered into the isothermal calorimeter preconditioned at 23 ± 0.05 °C. The total wet mixing time was less than 20 min to finish all 8 samples. The heat release was measured for 7 days in the calorimeter. The heat release values were normalized to the mass of binder in the paste. Triplicate testing on the samples from the same batch showed less than a 3% coefficient of variation (CoV) in the heat of hydration test.

Thermogravimetric analysis - Cementitious pastes were used for hydration products analysis on a TA Instruments SDT Q600 TGA. About 70 g of fresh paste was prepared as described above and loaded into three 10 ml cylindrical vials. After sealing, the vials were fixed onto a rotating cylinder at a speed of 20 rpm for 7 hours to avoid material and water segregation before being transferred into a 23 °C moist room. At 7, 28 and 56 days, the cylindrical vials were broken. The pastes were crushed and then submerged in IPA for solvent exchange to stop paste hydration. About 30-

50 mg of the paste was loaded into the TGA crucible and dried at 40 °C for 20 min prior to beginning the heating cycle. The temperature was then ramped at 10 °C/min from 40 °C to 900 °C in an inert N_2 atmosphere. To calculate the hydration products of the mixture, the mass losses in certain temperature ranges were measured using the tangential method described by Kim and Olek [29]. The mass loss between 50-600 °C corresponds to the bound water content of the paste [30]. The mass loss in the range of 380-460 °C indicates the water loss from $Ca(OH)_2$ [29,30]. The mass loss between 600-900 °C is due to the CO_2 release from $CaCO_3$ decomposition [29,30]. The carboaluminates decomposition will also create some mass loss at a lower temperature range, not captured in the CO_2 release mass loss [30]. These hydration products can be calculated based on the corresponding weight loss values. Triplicate testing on the samples from the same batch showed less than a 2% CoV in the TGA tests.

Setting time - The setting time of mixtures was determined according to ASTM C191. 650 g of the binder was mixed in trials to get the correct amount of water to reach normal consistency. Then, the normal consistency paste was transferred into the conical ring, and the setting time of the paste was recorded by a Humboldt Vicatronic automatic Vicat machine.

Compressive strength - Mortars were mixed according to ASTM C305 and cast into 50 mm mortar cubes according to ASTM C109. The binder powders were homogenized using a powder blender before mixing. A fixed w/b of 0.485 was adopted for all mixes. For each mixture, a total of 12 cubes were made, and 2 cubes were tested at 1, 3 and 7 days, and 3 cubes were tested at 28 and 56 days. The average value of each mixture is reported, and the CoV of the compressive strength results is less than 5% at all ages.

Bulk resistivity - Bulk resistivity measurements of the mixtures were carried out on the same cubes before compressive strength testing. The 50 mm mortar cubes were tested using the Giatec RCON resistivity meter according to ASTM C1876. The cubes were measured in a surface-dry state, and at a frequency of 1 kHz. Geometric corrections for cube specimen dimensions were applied to the measured values, and the average value of all 3 tested cubes is reported. The CoV of the measurements is less than 6% at all ages.

Accelerated mortar-bar test for alkali silica reaction (AMBT) - Mortar bars were cast and measured according to ASTM C305 and ASTM C1567. Three bars were cast for each mixture with gauge studs in both ends. The w/b and s/b were fixed at 0.47 and 1.90, respectively, for all mortar bars. The bars were cured in the moist room at 23 °C for 1 day before demolding, and then transferred into an 80 ± 2 °C water bath. After 24 h in 80 °C water, the bars were measured for the zero comparator readings. Then the bars were immersed in 1 M NaOH solution at 80 ± 2 °C, and the subsequent comparator readings of the bars were recorded. As per ASTM C1567, an expansion of more than 0.1% of the nominal gauge length at 14 days in the NaOH solution indicates potentially deleterious expansion due to ASR. The average expansion value of the 3 bars in one mixture is reported, and the CoV of the expansion measurements is below 2% for all mixtures.

RESULTS AND DISCUSSION

Heat of hydration

Fig. 2 shows the heat flow and heat release of the pastes with and without vaterite inclusion. The 25% fly ash binary paste (25F) reached the peak heat flow at 11.7 h after mixing. After replacing 10% fly ash with vaterite, the peak heat flow occurred at 10.8 h and reached a higher intensity. The highest peak of heat flow was caused by C_3S hydration, and the shoulder peak that occurred later was due to the C_3A reaction (When expressing cement phases, C = CaO, S = SiO_2, A = Al_2O_3, F = Fe_2O_3. For example, C_3A = $3CaO \cdot Al_2O_3$). Including 10% of vaterite to replace fly ash promoted the cementitious paste's C_3A reaction. The C_3A reaction shoulder peak occurred earlier than without vaterite. Similar reactions were seen in the slag-vaterite mixes, where the aluminate reaction peak was accelerated. For the two cement-slag-fly ash-vaterite systems, the acceleration by vaterite was more significant, with a much shorter induction period, shorter time to peak heat flow, and higher peak intensities. The C_3A shoulder peak happened in a faster and more intense way compared to the non-vaterite mixes. With both the main hydration peaks of silicates and aluminates being accelerated, the total heat release of pastes with vaterite inclusion was higher than their non-vaterite counterparts. The increase in total hydration heat was more obvious in the cement-slag-fly ash-vaterite quaternary pastes which only had 30-50% cement in the mixture. The vaterite-included quaternary mixtures had a higher and faster accelerating heat release value throughout the 7 days testing period, with a 9-10% increase at the end of 7 days. This suggested that 10% vaterite replacement of fly ash promoted more hydration reactions than cement blends with higher SCM amounts.

The acceleration of C_3A reactions was expected in the presence of vaterite. Due to its higher reactivity and solubility than calcite or limestone, vaterite may react faster with the aluminates at the beginning of the hydration and form carboaluminates while consuming monosulfate, thus stabilizing ettringite [3,8,20,31]. The additional aluminates provided by fly ash and slag to the system during their pozzolanic reaction and hydration further promoted the reaction of vaterite, and the synergistic effects between vaterite and aluminosilicate based SCMs can lead to improved mechanical properties over time [14,32,33]. The benefits offered by vaterite inclusion will be more significant when higher amounts of aluminosilicate based SCMs are present in the mixture.

Thermogravimetric analysis

Fig. 3 presents the TGA results of cementitious pastes with and without vaterite in four systems. Thermogravimetric analysis can be used to quantify hydration by measuring $Ca(OH)_2$ and bound water. In the hydration analysis, the paste mixtures without vaterite were compared with their 10% vaterite inclusion counterparts. The phase content calculations were normalized to the dry sample weight or anhydrous binder weight at 600 °C [34]. Between 7 and 56 days for all systems, the remaining $CaCO_3$ in the cementitious paste was reduced by up to 1% due to the vaterite reaction with the reactive alumina in the system. For the cement-fly ash-vaterite system, replacing fly ash with 10% vaterite increased the $Ca(OH)_2$ and bound water amount at 7 days, implying more hydration products were generated at early-ages. This was expected because the finer particle size vaterite ($d_{50} = 5.7$ μm) was replacing the coarser fly ash powder ($d_{50} = 23.3$ μm) and the early-age hydration was much accelerated by the nucleation of C-S-H on the vaterite surface. Fly ash is a slowly reacting material and does not provide much hydration benefits to blended cements at early-ages. As a more soluble polymorph of calcium carbonate, vaterite could provide more carbonate ions to react with the reactive alumina, and this can promote blended cements' early-age hydration and facilitate the reactive alumina dissolution from fly ash particles. These benefits in hydration products were not as significant at 28 or 56 days when the fly ash pozzolanic reaction gradually caught up. As for the cement-slag-vaterite systems, using 10% vaterite to replace slag did not enhance hydration as much as in the fly ash system. This was expected because vaterite was replacing a very fine ($d_{50} = 6.3$ μm) and reactive slag component in the blend. The noteworthy fact was that the overall bound water content of mixture 20S_10V was not reduced at both ages, compared to mixture 30S, indicating that the 10% vaterite replacement achieved similar hydration benefits as slag itself. The synergy between vaterite, slag, and cement allowed the reduction of slag, while maintaining similar amounts of hydration products through 28 days. In both cement-slag-fly ash-vaterite quaternary systems, the 10% vaterite inclusion increased the bound water content at 7 days by 16 to 23% and produced a slightly higher and lower amount of bound water at 28 days for 30S_10F_10V and 40S_20F_10V, respectively. The overall hydration in the quaternary systems was significantly promoted at early-ages, which was similar to the performance of the cement-fly ash-vaterite system.

As an indicator of degree of hydration, it's well known that the bound water of hydrated cements correlates well with mortar or paste strength at various ages [35,36]. Thus, if the bound water amount is increased in certain cement blends, the total amount of hydration products and the compressive strength will likely also be promoted. The positive linear correlation between paste bound water and the corresponding mortar strength was also shown in this study, illustrated in Fig. 4. Using 10% vaterite to replace fly ash in different systems increased the bound water content by about 20%, indicating a 20% higher overall degree of hydration. When replacing slag, the 10% vaterite did not compromise the overall degree of hydration. The benefits of vaterite came from both the physical effects such as shearing of the particles, increased water to clinker ratio, more nucleation of C-S-H on the vaterite surface, and the chemical reaction between vaterite and aluminates, resulting in the successful reduction of the SCM amount in the blended cements.

Setting time

Table 5 exhibits the initial setting time comparison between the cement pastes with and without vaterite. For the cement-fly ash-vaterite and cement-slag-vaterite systems, the inclusion of 10% vaterite reduced the setting time by 18 and 19 min, respectively. For the two cement-slag-fly ash-vaterite quaternary systems, the inclusion of 10% vaterite reduced the mixture's initial setting time by 50 and 118 minutes in the 30S_10F_10V and 40S_20F_10V systems, respectively. The inclusion of vaterite to replace fly ash and slag achieved a shorter initial setting time, especially when less cement was present. The setting time difference between non-vaterite and vaterite-included mixes was consistent with the measured time of the peak heat flow in the calorimetry test. A shorter time to peak heat flow indicates faster hydration reaction, and the accelerated hydration was attributed to the increased surface area for C-S-H to grow on due to vaterite inclusion, as evidenced by the TGA results. With a higher specific surface area, vaterite particles can provide more nucleation sites at early-ages of hydration than other SCMs or cement particles, thus

increasing the gel-space ratio in the hydration matrix structure and leading to a higher compressive strength [14]. Vaterite has a higher solubility and reactivity than other calcium carbonate polymorphs, and the more dissolved carbonate ions can contribute to a higher extent of reaction with aluminates, thus promoting the mixtures' overall degrees of hydration and forming more hydration products that can offer strength [20,23].

Mortar flow and compressive strength

Fig. 6 compares the compressive strength development between 0%, 5% and 10% vaterite inclusions in the four cementitious systems. The flow of mortar is an indicator of workability (listed in Table 3), and by replacing 10% fly ash or slag using the spherical vaterite, the flow was either maintained or increased, respectively. For the cement-slag-vaterite system, the 10% vaterite replacement improved the mortar flow by 9%. The spherical vaterite can be very effective in improving the workability of high-water demand mixtures. In terms of strength development, For the cement-fly ash-vaterite system, the 5% and 10% vaterite replacement of fly ash achieved a 30 to 40% higher 1-day strength, and a 19% to 31% higher 7-day strength. The higher strength of vaterite-containing mixtures was maintained through 56 days with about a 10% increase in strength compared to the cement blend without vaterite, 25F. In the cement-fly ash-vaterite system, the 10% vaterite replacement contributed more at early-ages and the 5% replacement showed a larger strength increase at later ages.

However, the replacement of a faster-reacting component, such as the fine slag, may not achieve similar improvements as replacing fly ash. For the cement-slag-vaterite system, the 5% vaterite replacement achieved the best performance up to 7 days. The strength was increased by more than 20% at 3 days and by about 8% at 7 days. At 28 days and 56 days, the vaterite replacement showed a less than 10% decrease on the strength compared to the slag-cement binary mixture. In the cement-slag-vaterite system, both 5% and 10% replacement levels showed similar benefits. Although vaterite can still offer early-age physical benefits and have synergy effects with slag, the improvement was not as significant as with fly ash replacement. The reduced hydration improvement in the slag ternary system is also in accordance with the calorimetry and TGA analysis.

For the cement-slag-fly ash-vaterite quaternary systems, the vaterite inclusion drastically improved the strength performance at early-ages, especially at the lower cement content. The 10% vaterite replacement of fly ash in the 50% cement mixtures, 30S_10F_10V, improved the early-age strength by 30% through 7 days, and the beneficial effects were much larger than the 5% vaterite replacement mixtures, 30S_15F_5V, through all ages. For the 30% cement mixtures, by including 10% vaterite, the 3-day strength was increased by 57%, and both 1- and 7-day strengths were increased by 30%. This is because with higher amounts of cement substitution with fly ash and slag, more reactive alumina from these SCMs is available to react with the vaterite. A higher vaterite replacement is more suitable for higher aluminosilicate based SCM amount systems, and such mixtures also have lower clinker factors. The co-substitution of vaterite and aluminosilicate based SCMs result in synergistic effects in blended cement. In both quaternary systems, the early-age strength benefited more from the vaterite addition than the late-age strength, which is consistent with its acceleration of early-age hydration reactions.

For all systems, the early-age strength improvement was most significant with a higher vaterite inclusion (10%). The improved early-age strength was in accordance with the heat evolution analysis from isothermal calorimetry, where the 10% vaterite not only increased the peak rate of hydration, but also shortened the induction time. It is known that the early-age strength correlates well with the heat of hydration [10,36–38], and both the quaternary systems showed significant increases in heats of hydration when replacing 10% fly ash with vaterite. The shortened setting time also agreed with the improved early-age strength of the cement-slag-fly ash-vaterite quaternary mixes. And the much shorter setting time and higher early-age performance would be beneficial for low temperature or winter construction. The significant improvement at early ages by vaterite was expected because the physical effects of increased C-S-H nucleation on the surface area of vaterite, increased water to clinker ratio, shearing action of particles, and improved packing are more predominant at early-ages and because the reactivity of vaterite promotes the formation of carboaluminate phases, providing more hydration products at early-ages. A previous study also confirmed that vaterite-included mixtures achieved the lowest porosity and highest solid volume in the cement paste comparing to its aragonite or calcite counterparts [23]. At later ages of 28 or 56 days, the 5-10% vaterite replacement in all systems achieved 89 to 119% of the original non-vaterite blended cements' strengths.

Bulk resistivity

Electrical resistivity or conductivity provides a rapid indication of a material's resistance to the penetration of fluids and dissolved aggressive ions, such as Cl^-, alkali, and SO_4^{2-}. Bulk electrical resistivity is a material property that depends on the pore structure, pore solution composition, degree of saturation of the specimen, and temperature of the specimen. A higher bulk resistivity value is generally indicative of a more durable material, with a higher resistance to penetration by chloride and other ions. From Table 6, all systems' bulk resistivities were improved by the inclusion of vaterite to differing degrees. When 5% vaterite was used to replace the slow reacting fly ash, the bulk resistivity was increased by 19% at 56 days in the cement-fly ash-vaterite system. For the cement-slag-vaterite systems, the 5% vaterite inclusion increased the 56-day bulk resistivity by 41%. In both low clinker factor quaternary systems, the bulk resistivity was improved significantly at both 28 and 56 days. In the 50% cement quaternary system, a 5-10% vaterite inclusion achieved a ≥75% higher bulk resistivity at 28 days, and a ≥39% higher value at 56 days. In the 30% cement quaternary system, a 5-10% vaterite inclusion improved the mortar's bulk resistivity by ≥91% at 28 days, and ≥63% at 56 days. Again, a higher vaterite replacement offered more benefits to higher aluminosilicate based SCM mixtures.

In the presence of vaterite, the reactions of clinker and SCMs were increased due to the continuous hydration reactions enhanced by the surface area of vaterite [14,33], and the dissolved carbonate ions reacting with the reactive alumina from the SCMs [7,20,23,39]. These effects lead to more hydration products formed over time and create a more tortuous pore structure. A refined pore structure and more hydration products, such as the interlayer structured carboaluminates [40], inhibit ion mobility and absorb ions, thus improving the electrical resistivity of the sample. With vaterite and SCM inclusion, both an increased pore refinement and a lower pore solution alkalinity were likely achieved, reducing the mass transport within the sample, thus increasing the electrical resistivity [5].

AMBT expansion

Fig. 8 shows the AMBT expansion of mortar bars after 14 days exposure of 80 °C alkaline solution. The corresponding ASTM standard C1567 states that an expansion less than 0.10% at 14 days of testing (16 days after casting) is likely to produce acceptable expansions when tested in concrete and to have a low risk of deleterious ASR expansion in field conditions. From the AMBT results, all the tested groups expanded much less than 0.10%, and the vaterite included mixtures showed a decreasing expansion trend while their non-vaterite counterparts had increasing expansion at the end of AMBT. This aligned with the bulk resistivity results which showed that at later ages, the durability benefits provided by vaterite addition were more obvious. For both cement-slag-fly ash-vaterite quaternary systems, the 10% fly ash reduction by vaterite inclusion did not reduce the mixture's ASR resistance. When replacing 10% fly ash with vaterite, the difference in expansion between the non-vaterite control and the vaterite-included mortar bars was negligible throughout the 14-day testing period. This supports that vaterite can be an effective material to supplement or replace fly ash or slag in blended cements.

CONCLUSIONS

This paper discusses the results and benefits of a 5-10% vaterite replacement of SCMs in certain blended cements. In a cement-fly ash blended cement, a 10% vaterite replacement of fly ash achieved a 40% higher strength at 1 day and maintained a consistently higher strength than the cement-fly ash blended cement control through 56 days. A 10% vaterite replacement of slag in a cement-slag blended cement achieved approximately 20% higher strength at 3 days. For a cement-slag-fly ash blended cement, a 10% replacement of fly ash with vaterite achieved approximately a 30-55% increase in strength through 7 days and a 50 to 110-minute reduction in initial setting. The bulk resistivity of the cement-slag-fly ash-vaterite quaternary mixtures were increased by 75-90% at 28 days by including vaterite, indicating that the vaterite containing blended cements should provide good durability. The alkali silica reaction test results confirmed the mortar durability and low expansion over the periods tested. Hydration analysis using isothermal calorimetry and thermogravimetry confirmed the accelerated early-age hydration reactions due to vaterite's physical and chemical benefits. The inclusion of vaterite accelerates both the main hydration peaks of silicates and aluminates. The total heat release of fly ash containing pastes with vaterite was higher than their non-vaterite counterparts. In an era of dwindling availability of traditional SCMs, vaterite shows the potential to extend those supplies and improve the overall performance of the resulting cement blends, which provides a solution to the cement and concrete industries to help achieve their sustainability goals.

ACKNOWLEDGMENTS

REFERENCES

[1]   I.H. Shah, S.A. Miller, D. Jiang, R.J. Myers, Cement substitution with secondary materials can reduce annual global CO2 emissions by up to 1.3 gigatons, Nat. Commun. 13 (2022) 1–11. https://doi.org/10.1038/s41467-022-33289-7.

[2]   M.G. Plaza, S. Mart, F. Rubiera, Cement Industry : State of the Art and Expectations, Energies. (2020). www.worldcementassociation.org/images/info-graphics/001-World-Wide-Cement-Production.pdf%0Awww.mdpi.com/journal/energies.

[3]   A.M. Ramezanianpour, R.D. Hooton, A study on hydration, compressive strength, and porosity of Portland-limestone cement mixes containing SCMs, Cem. Concr. Compos. 51 (2014) 1–13. https://doi.org/10.1016/j.cemconcomp.2014.03.006.

[4]   B. Lothenbach, G. Le Saout, E. Gallucci, K. Scrivener, Influence of limestone on the hydration of Portland cements, Cem. Concr. Res. 38 (2008) 848–860. https://doi.org/10.1016/j.cemconres.2008.01.002.

[5]   K.S.T. Chopperla, J.A. Smith, J.H. Ideker, The efficacy of portland-limestone cements with supplementary cementitious materials to prevent alkali-silica reaction, Cement. 8 (2022) 100031. https://doi.org/10.1016/j.cement.2022.100031.

[6]   K. Bharadwaj, O.B. Isgor, W.J. Weiss, Supplementary Cementitious Materials in Portland- Limestone Cements, ACI Mater. J. 119 (2022). https://doi.org/10.14359/51734356.

[7]   M.C.G. Juenger, R. Snellings, S.A. Bernal, Supplementary cementitious materials: New sources, characterization, and performance insights, Cem. Concr. Res. 122 (2019) 257–273. https://doi.org/10.1016/j.cemconres.2019.05.008.

[8]   F. Avet, K. Scrivener, Investigation of the calcined kaolinite content on the hydration of Limestone Calcined Clay Cement (LC3), Cem. Concr. Res. 107 (2018) 124–135. https://doi.org/10.1016/j.cemconres.2018.02.016.

[9]   F. Avet, X. Li, K. Scrivener, Determination of the amount of reacted metakaolin in calcined clay blends, Cem. Concr. Res. 106 (2018) 40–48. https://doi.org/10.1016/j.cemconres.2018.01.009.

[10]   Y. Wang, L. Burris, R.D. Hooton, C.R. Shearer, P. Suraneni, Effects of unconventional fly ashes on cementitious paste properties, Cem. Concr. Compos. 125 (2022) 104291. https://doi.org/10.1016/j.cemconcomp.2021.104291.

[11]   M. Kasaniya, M.D.A. Thomas, E.G. Moffatt, Cement and Concrete Research Pozzolanic reactivity of natural pozzolans , ground glasses and coal bottom ashes and implication of their incorporation on the chloride permeability of concrete, Cem. Concr. Res. 139 (2021) 106259. https://doi.org/10.1016/j.cemconres.2020.106259.

[12]   E. Berodier, K. Scrivener, Understanding the filler effect on the nucleation and growth of C-S-H, J. Am. Ceram. Soc. 97 (2014) 3764–3773. https://doi.org/10.1111/jace.13177.

[13]   T. Matschei, B. Lothenbach, F.P. Glasser, The role of calcium carbonate in cement hydration, Cem. Concr. Res. 37 (2007) 551–558. https://doi.org/10.1016/j.cemconres.2006.10.013.

[14]   Y. Dhandapani, M. Santhanam, G. Kaladharan, S. Ramanathan, Towards ternary binders involving limestone additions — A review, Cem. Concr. Res. 143 (2021). https://doi.org/10.1016/j.cemconres.2021.106396.

[15]   H. Mehdizadeh, K.H. Mo, T.C. Ling, CO2-fixing and recovery of high-purity vaterite CaCO3 from recycled concrete fines, Resour. Conserv. Recycl. 188 (2023) 106695. https://doi.org/10.1016/j.resconrec.2022.106695.

[16]   A.M. Ferreira, A.S. Vikulina, D. Volodkin, CaCO3 crystals as versatile carriers for controlled delivery of antimicrobials, J. Control. Release. 328 (2020) 470–489. https://doi.org/10.1016/j.jconrel.2020.08.061.

[17]   Z. Feng, T. Yang, S. Dong, T. Wu, W. Jin, Z. Wu, B. Wang, T. Liang, L. Cao, L. Yu, Industrially synthesized biosafe vaterite hollow CaCO3 for controllable delivery of anticancer drugs, Mater. Today Chem. 24 (2022) 100917. https://doi.org/10.1016/j.mtchem.2022.100917.

[18]   C.W. Hargis, I.A. Chen, M. Devenney, M.J. Fernandez, R.J. Gilliam, R.P. Thatcher, Calcium Carbonate Cement: A Carbon Capture, Utilization, and Storage (CCUS) Technique, Materials (Basel). (2021) 1–12.

[19]   J. Rodríguez-Sánchez, T. Liberto, C. Barentin, D.K. Dysthe, Mechanisms of phase transformation and creating mechanical strength in a sustainable calcium carbonate cement, Materials (Basel). 13 (2020). https://doi.org/10.3390/MA13163582.

[20]   C.W. Hargis, A. Telesca, P.J.M. Monteiro, Calcium sulfoaluminate (Ye'elimite) hydration in the presence of gypsum, calcite, and vaterite, Cem. Concr. Res. 65 (2014) 15–20. https://doi.org/10.1016/j.cemconres.2014.07.004.

[21]   P.J.M. Monteiro, L. Clodic, F. Battocchio, W. Kanitpanyacharoen, S.R. Chae, J. Ha, H.R. Wenk, Incorporating carbon sequestration materials in civil infrastructure: A micro and nano-structural analysis, Cem. Concr. Compos. 40 (2013) 14–20. https://doi.org/10.1016/j.cemconcomp.2013.03.013.

[22]   C.W. Hargis, Advances in Sustainable Cements, UC Berkeley Electronic Theses and Dissertations, 2013.

[23]   D. Zhao, J.M. Williams, A.H.A. Park, S. Kawashima, Hydration of cement pastes with calcium carbonate polymorphs, Cem. Concr. Res. 172 (2023). https://doi.org/10.1016/j.cemconres.2023.107214.

[24]   O. Cherkas, T. Beuvier, F. Zontone, Y. Chushkin, L. Demoulin, A. Rousseau, A. Gibaud, On the kinetics of phase transformations of dried porous vaterite particles immersed in deionized and tap water, Adv. Powder Technol. 29 (2018) 2872–2880. https://doi.org/10.1016/j.apt.2018.08.008.

[25]   P. Chen, J. Wang, L. Wang, Y. Xu, X. Qian, H. Ma, Producing vaterite by CO2 sequestration in the waste solution of chemical treatment of recycled concrete aggregates, J. Clean. Prod. 149 (2017) 735–742. https://doi.org/10.1016/j.jclepro.2017.02.148.

[26]   C.W. Hargis, R.J. Gilliam, Compositions, methods, and systems to form vaterite with magnesium oxide, US 2023/0099641 A1, 2022. https://patentimages.storage.googleapis.com/24/ba/b9/64edf49839fe31/US20220340486A1.pdf.

[27]   M. Devenney, M. Fernandez, I. Chen, C. Guillaume, Methods and systems for utilizing carbide lime or slag, US 9,902,652 B2, 2018.

[28]   M. joseph Weiss, R.J. Gilliam, Methods and Systems For Treatment of Lime to Form Vaterite, US 11577965, 2023.

[29]   T. Kim, J. Olek, Effects of sample preparation and interpretation of thermogravimetric curves on calcium hydroxide in hydrated pastes and mortars, Transp. Res. Rec. 2290 (2012) 10–18. https://doi.org/10.3141/2290-02.

[30]   R. Bottom, Thermogravimetric Analysis, Princ. Appl. Therm. Anal. (2008) 87–118. https://doi.org/10.1002/9780470697702.ch3.

[31]   K. De Weerdt, K.O. Kjellsen, E. Sellevold, H. Justnes, Synergy between fly ash and limestone powder in ternary cements, Cem. Concr. Compos. 33 (2011) 30–38. https://doi.org/10.1016/j.cemconcomp.2010.09.006.

[32]   M. Antoni, J. Rossen, F. Martirena, K. Scrivener, Cement substitution by a combination of metakaolin and limestone, Cem. Concr. Res. 42 (2012) 1579–1589. https://doi.org/10.1016/j.cemconres.2012.09.006.

[33]   A. Arora, G. Sant, N. Neithalath, Ternary blends containing slag and interground/blended limestone: Hydration, strength, and pore structure, Constr. Build. Mater. 102 (2016) 113–124. https://doi.org/10.1016/j.conbuildmat.2015.10.179.

[34]   F. Deschner, F. Winnefeld, B. Lothenbach, S. Seufert, P. Schwesig, S. Dittrich, F. Goetz-Neunhoeffer, J. Neubauer, Hydration of Portland cement with high replacement by siliceous fly ash, Cem. Concr. Res. 42 (2012) 1389–1400. https://doi.org/10.1016/j.cemconres.2012.06.009.

[35]   S. Ramanathan, M. Croly, P. Suraneni, Comparison of the effects that supplementary cementitious materials replacement levels have on cementitious paste properties, Cem. Concr. Compos. 112 (2020) 103678. https://doi.org/10.1016/j.cemconcomp.2020.103678.

[36]   S. Kucharczyk, M. Zajac, C. Stabler, R.M. Thomsen, M. Ben Haha, J. Skibsted, J. Deja, Structure and reactivity of synthetic CaO-Al2O3-SiO2 glasses, Cem. Concr. Res. 120 (2019) 77–91. https://doi.org/10.1016/j.cemconres.2019.03.004.

[37]   D.P. Bentz, T. Barrett, I. De la Varga, W.J. Weiss, Relating compressive strength to heat release in mortars, Adv. Civ. Eng. Mater. 1 (2012) 20120002. https://doi.org/10.1520/acem20120002.

[38]   T. Baran, P. Pichniarczyk, Correlation factor between heat of hydration and compressive strength of common cement, Constr. Build. Mater. 150 (2017) 321–332. https://doi.org/10.1016/j.conbuildmat.2017.06.025.

[39]   K. Scrivener, A. Favier, Investigation of Ternary Mixes Made of Clinker Limestone and Slag or Metakaolin: Importance of Reactive Alumina and Silica Content, RILEM Bookseries. (2015) 545–546. https://doi.org/10.1007/978-94-017-9939-3.
[40]   F. Georget, B. Lothenbach, W. Wilson, F. Zunino, K.L. Scrivener, Stability of hemicarbonate under cement paste-like conditions, Cem. Concr. Res. 153 (2022) 106692. https://doi.org/10.1016/j.cemconres.2021.106692.

Table 1 - LOI (%), d_{50} values (μm), density (g/cm^3), and **surface** area (m^2/g) of the raw materials.

Material	LOI	d_{50}	density	surface area
Cement	1.7	12.7	3.2	1.3
Fly ash	0.6	23.3	2.1	2.3
Slag	1.4	6.3	3.0	1.5
Vaterite	43.5	5.7	2.5	5.5

Table 2 - Mixture proportions of cementitious pastes for hydration analysis given for 100 g of binder (w/b = 0.6).

Mixture	Cement (g)	Fly ash (g)	Slag (g)	Vaterite (g)	Water (g)
25F	75	25	0	0	60.0
15F_10V	75	15	0	10	60.0
30S	70	0	30	0	60.0
20S_10V	70	0	20	10	60.0
30S_20F	50	20	30	0	60.0
30S_10F_10V	50	10	30	10	60.0
40S_30F	30	30	40	0	60.0
40S_20F_10V	30	20	40	10	60.0

Table 3 - Mixture proportions of all mortar cubes given for 100 g of binder (w/b = 0.485, s/b = 2.75).

Mixture	Cement (g)	Fly ash (g)	Slag (g)	Vaterite (g)	Sand (g)	Water (g)	Flow (%)
25F	75	25	0	0	275	48.5	115
20F_5V	75	20	0	5	275	48.5	118
15F_10V	75	15	0	10	275	48.5	116
30S	70	0	30	0	275	48.5	106
25S_5V	70	0	25	5	275	48.5	105
20S_10V	70	0	20	10	275	48.5	115
30S_20F	50	20	30	0	275	48.5	114
30S_15F_5V	50	15	30	5	275	48.5	111
30S_10F_10V	50	10	30	10	275	48.5	114
40S_30F	30	30	40	0	275	48.5	118
40S_25F_5V	30	25	40	5	275	48.5	116
40S_20F_10V	30	20	40	10	275	48.5	119

Table 4 - Mixture proportions of mortar bars in ASTM 1567 accelerated mortar bar test given for 100 g of binder (w/b = 0.47, s/b = 1.90).

Mixture	Cement (g)	Fly ash (g)	Slag (g)	Vaterite (g)	Reactive aggregate (g)	Water (g)
25F	75	25	0	0	190	47
15F_10V	75	15	0	10	190	47
30S	70	0	30	0	190	47
20S_10V	70	0	20	10	190	47
30S_20F	50	20	30	0	190	47
30S_10F_10V	50	10	30	10	190	47
40S_30F	30	30	40	0	190	47
40S_20F_10V	30	20	40	10	190	47

Table 5 - The initial setting time of cementitious pastes with and without vaterite in four systems.

Mixture	Initial setting time (min)
25F	223
20F_5V	221
15F_10V	205
30S	177
25S_5V	171
20S_10V	158
30S_20F	275
30S_15F_5V	270
30S_10F_10V	225
40S_30F	410
40S_25F_5V	350
40S_20F_10V	302

Table 6 - Bulk resistivity development of blended cement mortars with and without vaterite.

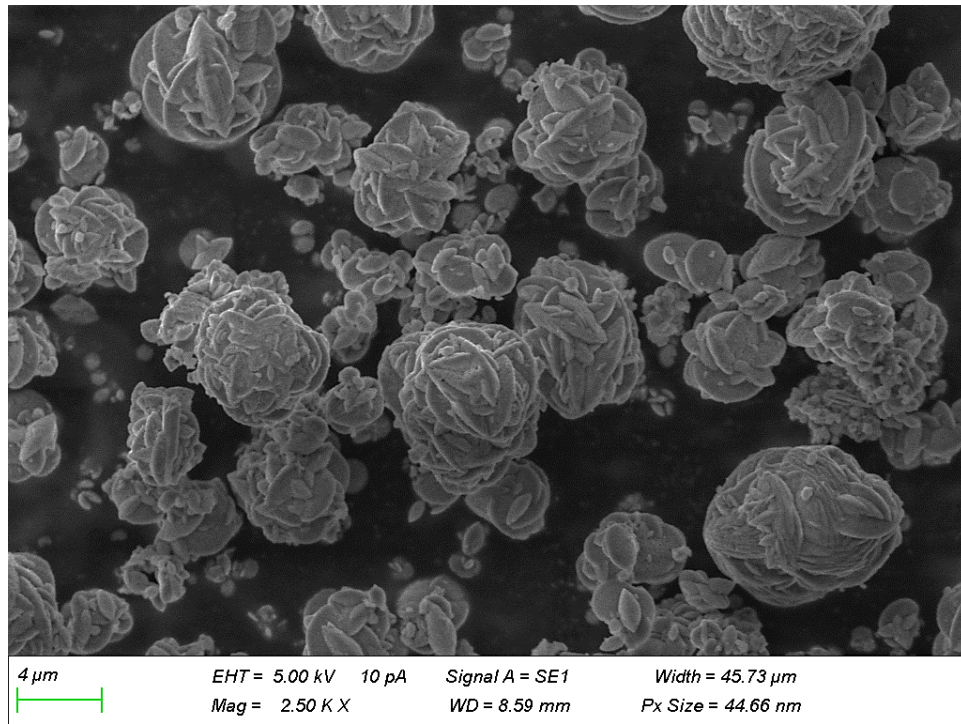| Mixture	28 days (Ohm*m)	56 days (Ohm*m)
25F	50.0	78.2
20F_5V	55.2	92.8
15F_10V	51.9	78.7
30S	75.3	75.0
25S_5V	93.3	106.0
20S_10V	83.0	91.2
30S_20F	81.5	130.8
30S_15F_5V	144.7	200.5
30S_10F_10V	142.5	181.8
40S_30F	134.7	203.0
40S_25F_5V	268.2	338.8
40S_20F_10V	257.7	330.7

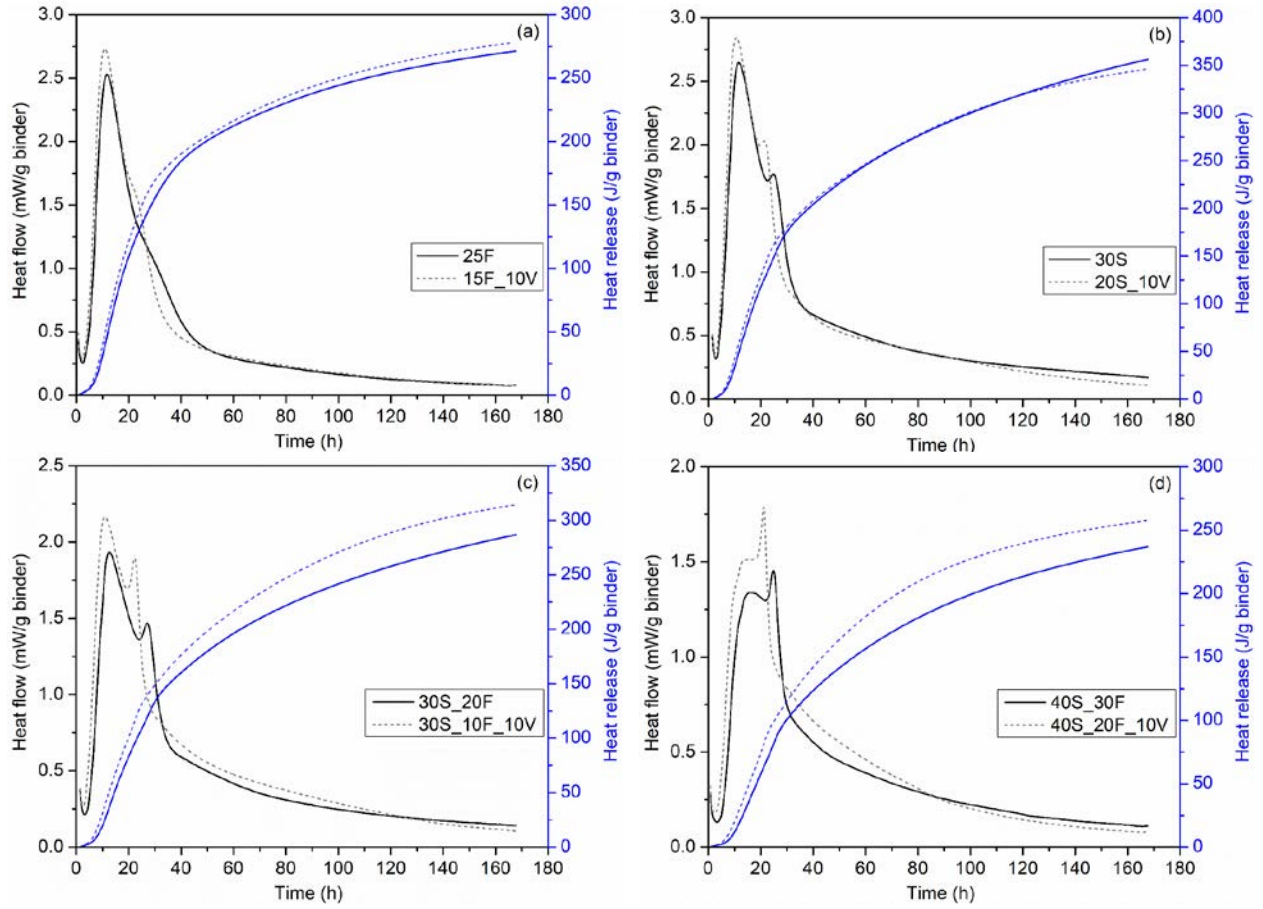**Fig.1** - SEM image of the vaterite particles.

Fig. 2 - Heat flow and cumulative heat release of cementitious pastes with and without vaterite.
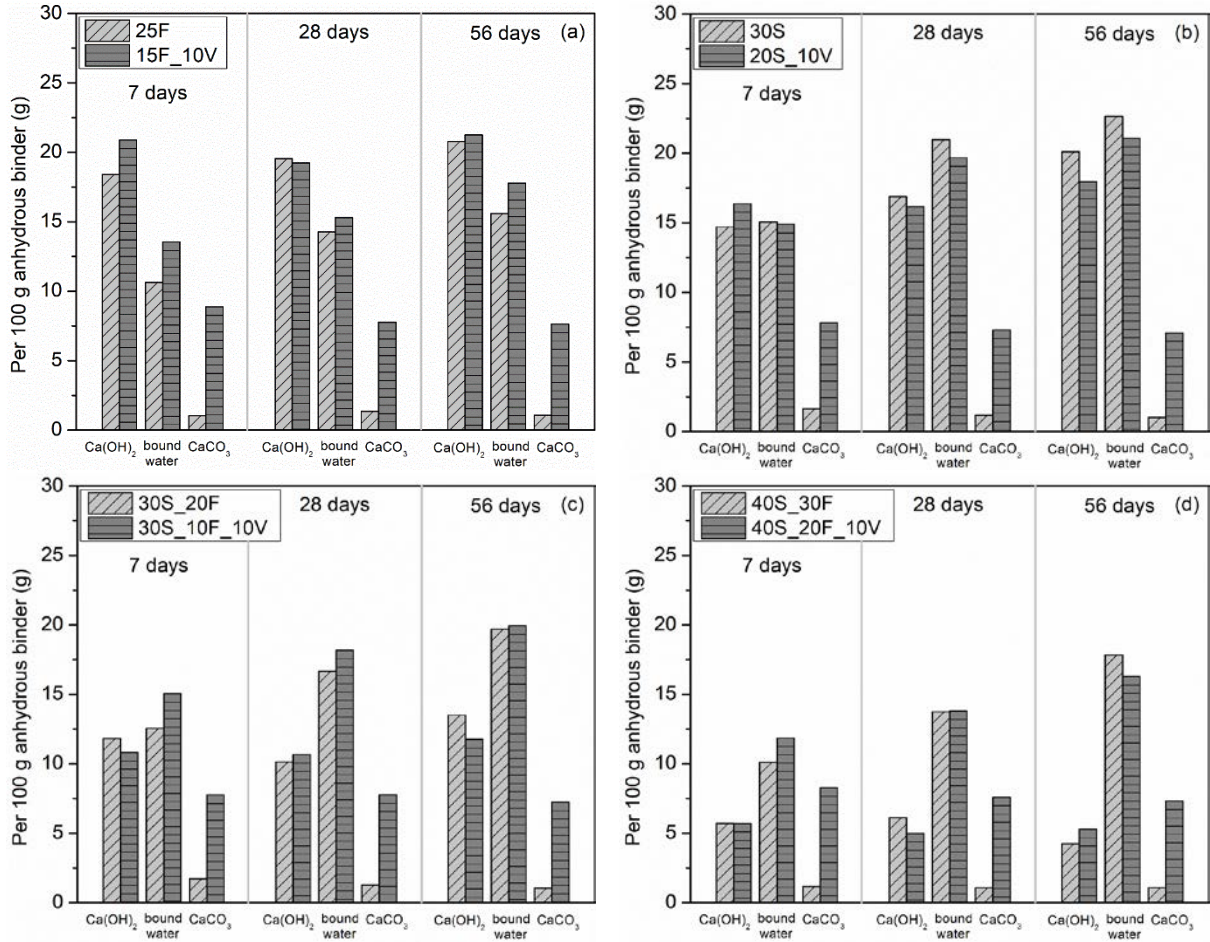
Fig. 3 - Thermogravimetric analysis of cement paste hydration products with and without vaterite in four systems.
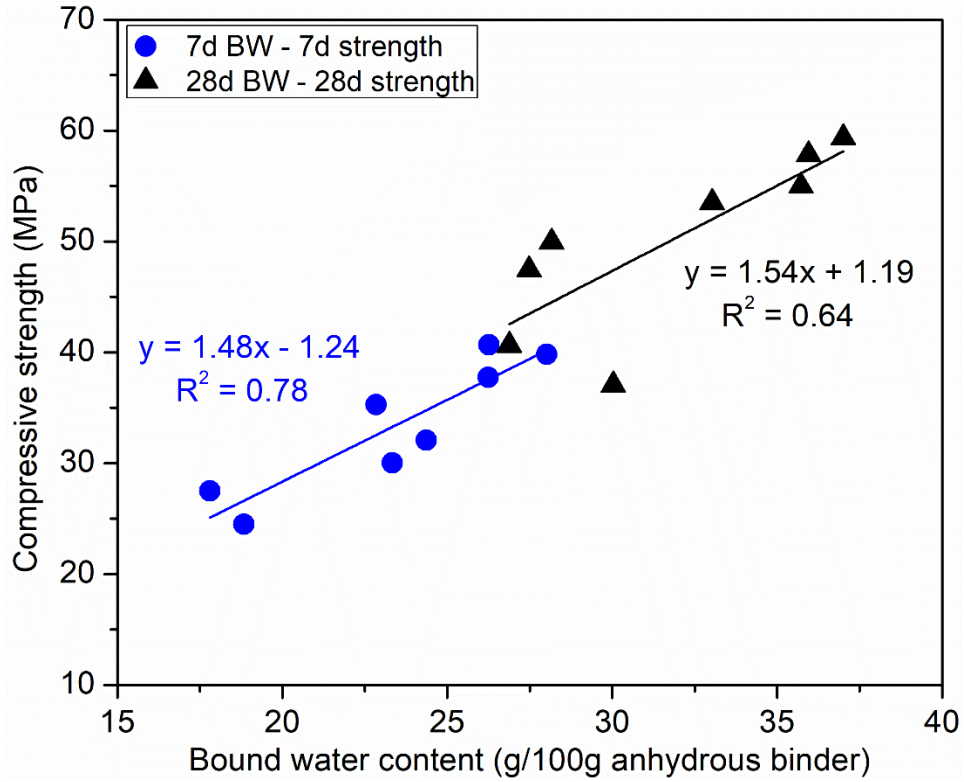
Fig. 4 - The correlations between cementitious paste 7- and 28-day bound water content (BW) and the corresponding mortars' 7- and 28-day compressive strength.
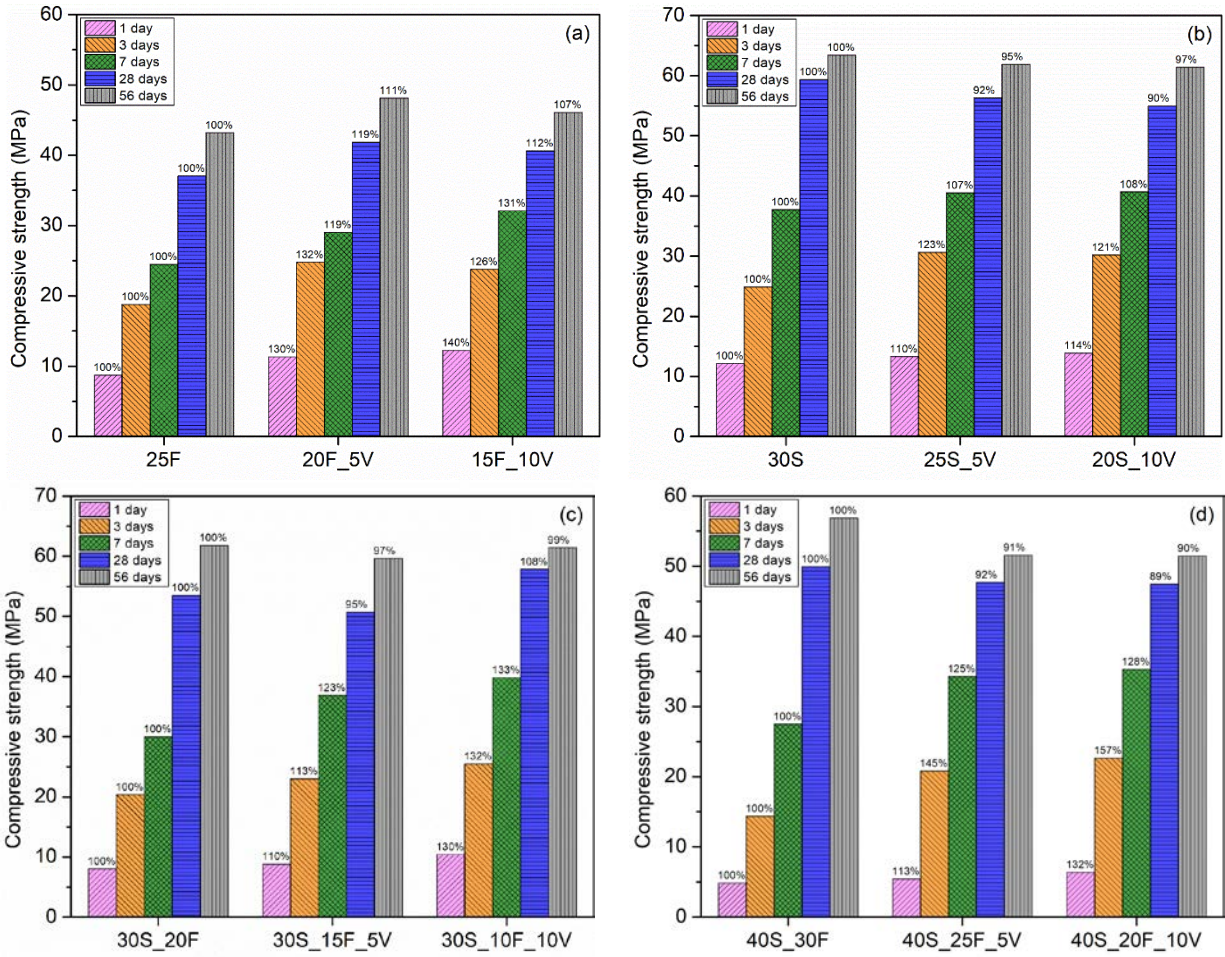
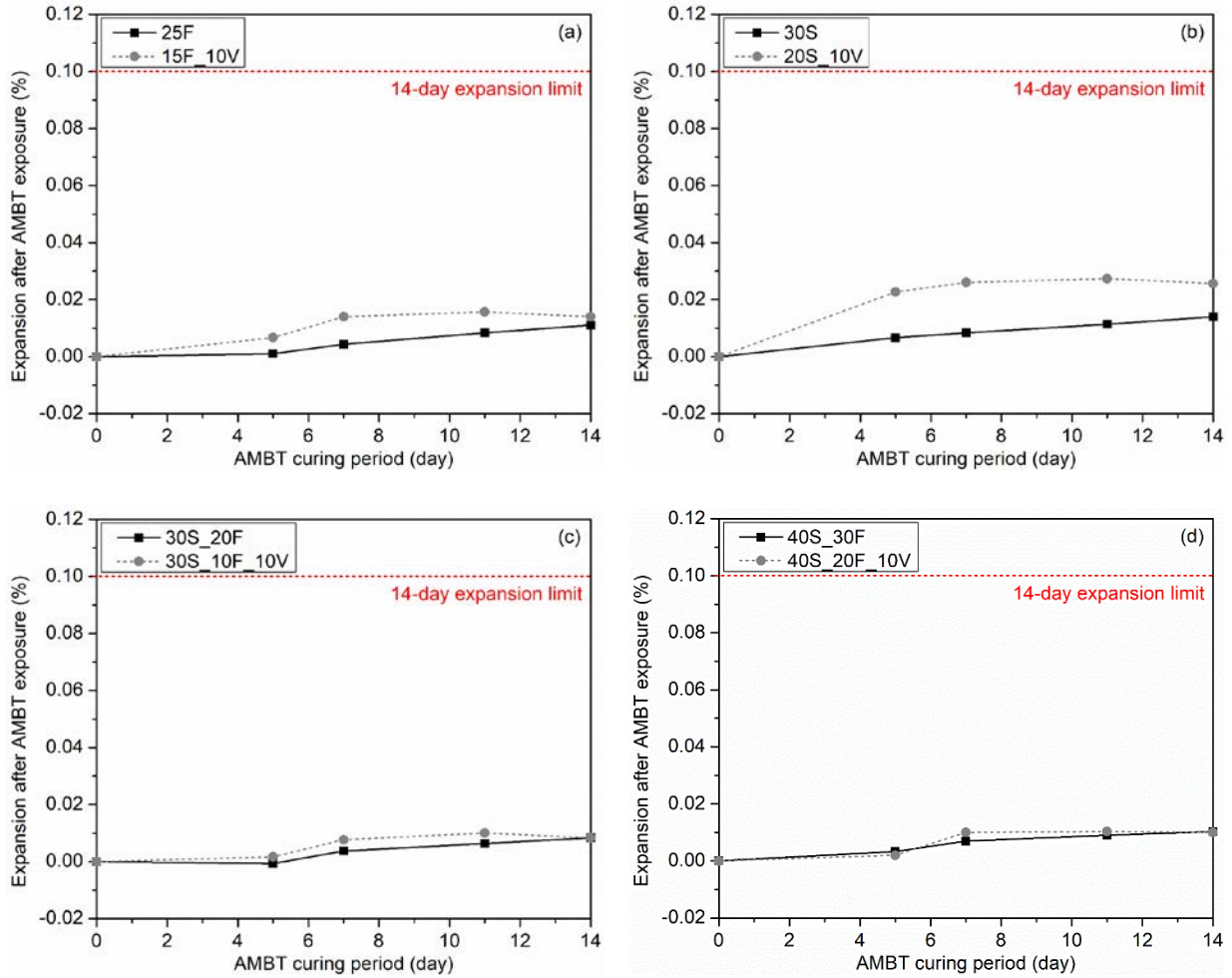**Fig. 5** - The strength development of blended cement mortars with and without vaterite.

Fig. 6 - The AMBT expansion of mortar bars with and without vaterite.